Emergent properties of organic matter decomposition by soil enzymes

Bin Wang[a,*], Steven D. Allison[a,b]

[a] Department of Ecology and Evolutionary Biology, University of California, Irvine, CA, USA
[b] Department of Earth System Science, University of California, Irvine, CA, USA

ARTICLE INFO

ABSTRACT

Plant residues and soil organic matter are predominantly decomposed by exoenzymes. Many soil carbon models now represent enzymatic decomposition, but the mathematical formulation of this process has been debated over the last 15 years. Some models apply the traditional "forward" Michaelis-Menten equation to represent enzyme kinetics, whereas others apply the "reverse" Michaelis-Menten equation, which assumes that kinetic rates saturate at high enzyme concentrations. Recently the equilibrium chemistry approximation (ECA) has been proposed as an alternative to both Michaelis-Menten formulations. However, because of methodological limitations, *in-situ* enzyme kinetics—especially in the context of soil system heterogeneity—have been difficult to verify experimentally. Therefore, the overarching goal of our study was to evaluate different enzyme kinetic formulations using model-based evidence at microbial to ecosystem scales. We used a spatially explicit individual- and trait-based microbial model, DEMENT, to circumvent methodological challenges. Although DEMENT assumes forward Michaelis-Menten kinetics at local scales, at the grid scale we found saturating relationships between degradation rate and both substrate concentrations and enzyme concentrations that fit the forward and reverse Michaelis-Menten equations, respectively, at specific successional stages during decomposition. Although forward and reverse Michaelis-Menten equations emerged under some conditions, only the ECA adequately represented decay rates emerging from the spatial-temporal variation in substrate and enzyme concentrations throughout the decomposition process. Our results support a more widespread adoption of the ECA equation in soil biogeochemical modelling at ecosystem scales.

1. Introduction

Decomposition of plant residues and soil organic matter is a fundamental process of regenerating compounds that can be used by plants and microbes. Carbon dioxide release by decomposition is integral to biosphere-atmosphere interactions in the Earth system. Exoenzymes influence this decomposition process by catalyzing substrate transformations (e.g., Sinsabaugh et al., 2008), although a variety of non-microbial processes can also contribute (Wang et al., 2017). Because enzymes are responsible for substrate degradation, an intuitive question thus arises: what is the relationship between organic matter decomposition rate and enzyme concentration? This kinetic relationship is critical for modelling decomposition rates and fluxes of carbon and nutrients between the biosphere and atmosphere.

Studies relating decomposition of organic matter/plant detritus to many environmental factors have a long history starting in the early 1930s (see reviews of Manzoni and Porporato, 2009; Wieder et al., 2015). However, an integration of enzymes into the quantitative representation of decomposition did not exist until the early 1990s. Until

then, first-order equations were used with relatively little attention to microbial activity and enzymes [but see Parnas (1975)]. Even in the early stages of accounting for enzymes, first-order equations derived from empirical relationships of decay versus enzyme activity were used (e.g., Sinsabaugh et al., 1992, 1994; Moorhead et al., 1996).

A more mechanistic description was borrowed from the enzymatic chemistry field as proposed by Michaelis and Menten (1913):

$$V = \frac{k_{cat}\, E_0\, S_0}{K_m + S_0} \tag{1}$$

where E_0 and S_0 represent enzyme and substrate concentration, respectively, k_{cat} represents the enzyme catalytic constant, and K_m denotes the concentration of S at which V is one half V_{max}. It is noteworthy that the earliest applications of the Michaelis-Menten relationship in microbial decomposition date back to the 1940s describing microbial growth in chemostats (Monod, 1942). This relationship has now become commonly applied to the kinetics of enzyme-driven soil organic matter degradation (e.g., Roberts, 1977; Manzoni and Porporato, 2009; Wieder et al., 2014).

However, debate has arisen over the application of the Michaelis-Menten equation since the proposal of the so-called 'reverse' Michaelis-Menten equation by Schimel and Weintraub in 2003 for soil carbon and nitrogen modelling:

$$V = \frac{k_{cat} S_0 E_0}{K_m + E_0} \tag{2}$$

'Reverse' refers to the reaction rate saturating with increasing enzyme instead of substrate as in the forward equation. This modification is based on Langmuir adsorption isotherm theory which posits that substrate binding sites may become limiting as enzyme concentration increases (Schimel and Weintraub, 2003). To address a similar issue, the reverse equation has been suggested in the field of catalytic chemistry as well (e.g., Borghans et al., 1996; Tzafriri, 2003; Bajzer and Strehler, 2012; Kari et al., 2017). Over the past decade, researchers have proposed additional applications of the reverse equation (e.g., Moorhead et al., 2012; Sulman et al., 2014; Wieder et al., 2015) and conducted theoretical explorations of its rationale in soil organic matter modelling (e.g., Wang and Post, 2013; Tang, 2015; Moorhead and Weintraub, 2018). Over the past 15 years, biogeochemical models with different objectives and scales have applied one of the two equations depending on their developers' preferences and perspectives (see review by Wieder et al., 2015).

Recently, Tang and Riley (2013) proposed a third formulation of enzyme kinetics known as the equilibrium chemistry approximation (ECA):

$$V = \frac{k_2 S E}{k_m + S + E} \tag{3}$$

where k_2 and k_m refer to the maximum product genesis rate and the Michaelis-Menten constant, respectively. Tang and Riley (2013) derived the ECA from the first-order approximation of the full equilibrium chemistry formulation of a consumer–substrate network that can account for multiple consumers and multiple substrates. The ECA has been argued to be more general and therefore preferable to forward or reverse Michaelis-Menten kinetics (Tang, 2015). Still, selecting the best kinetic model in soil organic matter modelling has been hindered due to the difficulty of measuring enzyme kinetics under in-situ soil conditions, which are very heterogeneous in space and time.

To circumvent these limitations, we used a spatially explicit individual- and trait-based microbial modelling framework, DEMENT (Allison, 2012), to analyze enzyme kinetic equations in the context of simulated spatial-temporal heterogeneity. With this model-based evidence, we find, for the first time, that in addition to being a more general kinetic formulation, the ECA (Eq. (3)) is best able to represent substrate degradation rates emerging from heterogeneous soil environments. This result offers promise that the ECA equation could be widely adopted for simulating large-scale soil organic matter decomposition in Earth system models.

2. Methods

2.1. Model description

DEMENT (DEcomposition Model of ENzymatic Traits) is a spatially explicit individual- and trait-based microbial model that simulates litter decomposition as an outcome of the emergent behavior of microbial systems integrating processes from both individual cell-level physiology and community-level interactions (Allison, 2012). A microbial community composed of multiple taxa can be initiated with a random distribution on a spatial grid. In our study, the grid is 100×100, with each grid box approximately 1–10 µm on a side. During an explicit simulation of physiological metabolism and ecological interactions, microbes grow, die, reproduce, and disperse on the grid. Physiology is governed by trait distributions and tradeoffs, for example among enzyme production rate and enzyme kinetic parameters. Taxa produce

constitutive and inducible enzymes as a fraction of standing biomass and resource uptake, respectively. These enzymes explicitly degrade substrates of different types following the rule that all enzymes degrade at least one substrate and all substrates are degraded by at least one enzyme. Substrate degradation rates are calculated within each grid box using the forward Michaelis-Menten equation (Eq. (1)). A more detailed description and applications of this model are referred to Allison (2012) and Allison and Goulden (2017). The required input parameters of this model are listed in Table A1 in the Appendix. The source code of the DEMENT version used in this study written in the R programming language is available on GitHub (https://github.com/stevenallison).

2.2. Modelling setup and experiments

We set up DEMENT with only one bacterial taxon (simplifying the kinetic analysis from disturbances including ecological interactions) and specified an occupancy probability of 0.01 in each grid box of the 100×100 spatial grid. Following random placement of bacterial cells, 109 grid boxes were occupied by the taxon which produced a maximum of 30 different enzymes. Substrates (12 types in total including dead microbes and inactivated enzymes; see Table A2 in the Appendix for their initial amounts) were initialized homogeneously on the spatial grid to be decomposed by the taxon with different enzymes.

With the setup of DEMENT as described above, a series of enzyme manipulation simulations were conducted. Because enzyme production rates can vary across ecosystems, microbial taxa, and environmental conditions, we tested the model sensitivity to varying rates of constitutive and inducible enzyme production (expressed by parameters of EnzProdConstit and EnzProdInduce in the model, respectively; see Table A3 in the Appendix for a list of simulated rates). All simulations with differing enzyme production rates were driven by a constant temperature of 15 °C without water stress for 300 days (long enough to see dramatic system changes in substrate and enzyme concentrations). All other parameter values are listed in Table A1 in the Appendix.

2.3. Data analyses

Using the simulation outputs, we analyzed substrate degradation rates as a function of substrate and/or enzyme concentration. Note that different substrates were targeted by different enzymes but showed qualitatively similar spatial and temporal patterns of degradation. Also, different enzyme production rates did not alter the qualitative patterns of substrate degradation. Therefore, we selected cellulose dynamics at an intermediate enzyme production rate (15×10^{-5} mg C mg^{-1} day^{-1} for both constitutive and inducible production) for comprehensive analyses of enzyme kinetic relationships.

To determine how well enzyme kinetic equations captured substrate degradation rates at the whole grid scale, simulation data from every grid box on three different days (140, 160, and 200; chosen to capture the temporal variation) were extracted to examine relationships between degradation rate and both substrate and enzyme concentration by fitting the forward equation (Eq. (1)), the reverse equation (Eq. (2)), or the ECA equation (Eq. (3)). To further examine the overall performance of the different equations, a 'time-for-space' substitution approach was applied by plotting all points together from 5 different days (40, 80, 120, 160, and 200, each representing a different stage in the successional trajectory of substrate decay) to examine the relationship between degradation rate and both substrate and enzyme concentrations. Lastly, cellulose degradation rate and substrate and enzyme concentrations averaged over the spatial grid on each day were used to examine the degradation rate as a function of both substrate and enzyme concentrations (summed over the 3 enzymes shown in Table A4 in the Appendix). These data were fitted with the ECA equation (Eq. (3)).

All non-linear regression analyses in this study were completed by obtaining the best fit between DEMENT output data and corresponding
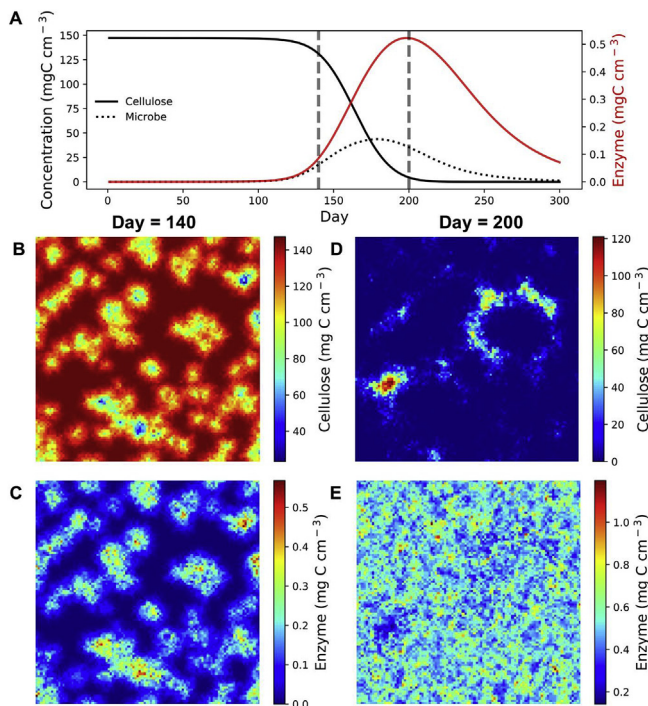
Fig. 1. Temporal dynamics and spatial pattern of cellulose and corresponding enzyme abundance on the 100×100 spatial grid. A) the temporal dynamics of cellulose and enzyme concentrations averaged over the spatial grid, as well as the trajectory of mean microbial biomass density, over 300 days with enzyme production rates of 15×10^{-5} mg C mg^{-1} day^{-1} for both constitutive and inducible production. Spatial distributions are shown for day 140 (**B, C**) and day 200 (**D, E**). Note three different enzymes are responsible for the degradation of cellulose in the simulation (see kinetic parameters in Table A4 in the Appendix).

models (Eqs. 1-3) using a nonlinear least-squares approach with the Gauss-Newton algorithm of the *nls()* function in the R programming language. We calculated RMSE (root mean squared error) to quantify model fit.

3. Results

3.1. Spatial pattern and temporal dynamics of substrate and enzymes

Cellulose—our example substrate—declined gradually until around day 120 when its concentration started to decline sharply before nearly disappearing over the next 80 days (Fig. 1A). In contrast, enzyme concentrations lagged behind biomass to reach a peak value of ~ 0.5 C cm^{-3} on day 200, after which the enzyme concentrations started to decline (Fig. 1A). The enzyme peak lags the biomass peak because high inducible enzyme production happens after increased monomer uptake from the biomass-driven peak in constitutive enzyme production. On day 140, the cellulose concentration varied from < 40 to ~ 140 mg C cm^{-3}, whereas the enzyme concentration ranged from zero to as high as ~ 0.5 mg C cm^{-3} (Fig. 1B and C). A maximum biomass: substrate ratio of 2631.733 was reached on day 281, and a maximum enzyme: biomass ratio of 0.055 was reached on day 300. Locally high enzyme concentrations resulted in substrate 'holes' with low substrate concentrations. These 'holes' deepened and expanded (Fig. 1D) as enzymatic degradation increased (Fig. 1E). Over time, reproduction and dispersal of microbial cells across the grid led to an expansion of areas with high enzyme concentrations.

3.2. Relationships between rates and enzyme/substrate concentrations over the spatial grid

To test the applicability of the forward and reverse equations, the relationships between degradation rate and both enzyme and substrate concentrations over the spatial grid were analyzed on selected days by fitting the forward equation (Fig. 2A,C,E) or reverse equation (Fig. 2B,D, F). On day 140, the reverse equation provided a good fit to substrate degradation rates (Fig. 2B), whereas the forward equation did not (Fig. 2A). By day 160, the reverse equation fit the degradation rate to some extent (Fig. 2D), while the forward equation apparently did not (Fig. 2C). By day 200, the forward equation fit the substrate degradation rate (Fig. 2E), whereas the reverse equation did not (Fig. 2F).

When spatial data were combined across time from four selected days (Fig. 3), most of the data points clustered around areas with high substrate concentrations (nearly 150 mgC cm^{-3}) and near-zero rate (from early in the simulation) or around areas of fairly low substrate
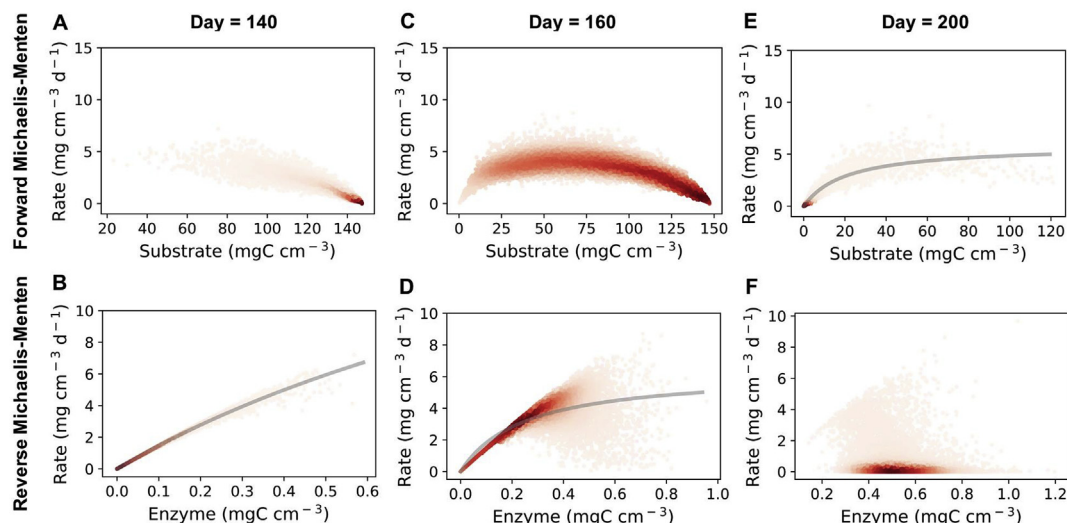

Fig. 2. Degradation rate versus enzyme and substrate concentration over the 100×100 spatial grid on different days. Data shown are extracted from every grid box on days 140, 160, and 200. High intensity of color denotes higher density of points based on kernel density distribution. Lines in **B** (Vmax: 24.895 mg substrate mg^{-1} enzyme d^{-1}; Km: 1.595 mg cm^{-3}) and **D** (Vmax: 6.324 mg substrate mg^{-1} enzyme d^{-1}; Km: 0.248 mg cm^{-3}) show the best fits of the reverse equation (Eq. (2)), whereas E (Vmax: 5.862 mg substrate mg^{-1} enzyme d^{-1}; Km:20.781 mg cm^{-3}) shows the best fit of the forward equation (Eq. (1)). Neither model fits in A, C, and F. (For interpretation of the references to color in this figure legend, the reader is referred to the Web version of this article.)
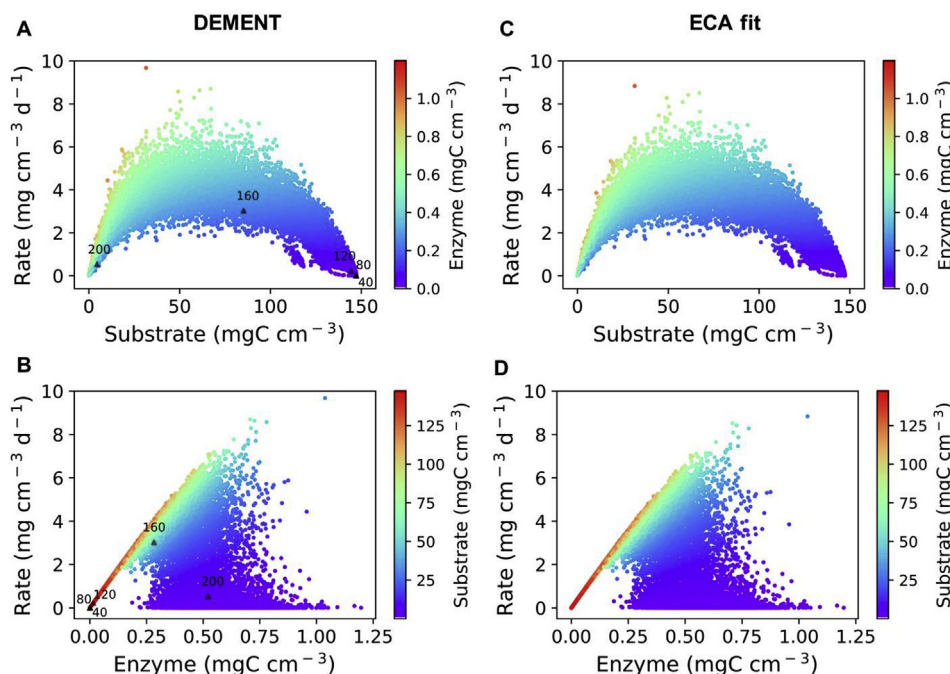
Fig. 3. Degradation rate versus substrate and enzyme concentration over the 100×100 spatial grid with data from specific dates plotted together. Points in A, B represent grid box data on days 40, 80, 120, 160, and 200 from the simulation with enzyme production rates of 15.0×10^{-5} mg C mg^{-1} day^{-1} (both constitutive and inducible). Black triangles denote the means for each day. Panels **C** and **D** show the best fit of the ECA equation (Eq. (3)) to data from panels **A** and **B**, with $k_2 = 18.722$ mg substrate mg^{-1} enzyme d^{-1} and $k_m = 36.722$ mg cm^{-3} (RMSE = 0.026 mg cm^{-3} d^{-1}). Different colors denote enzyme (**A,C**) or substrate concentration (**B,D**). (For interpretation of the references to color in this figure legend, the reader is referred to the Web version of this article.)

concentration and rate (from late in the simulation) (see Fig. A1A for the density of these data points). For rate versus enzyme, most of the data points clustered around areas with low enzyme concentrations and decay rates (from the early stage of the simulation) or around areas with moderate enzyme concentration (around 0.6 mgC cm^{-3}) and zero degradation rates (later in the simulation) (see Fig. A1B for the density of these data points). With these combined data from multiple days, both the reverse and forward equations failed to capture most of the spatial variation across the grid or even the daily grid averages (Fig. 3A and B). Specifically, the reverse equation failed to capture the low average degradation rate on day 200, and the forward equation failed to capture low average values early in the simulation (days 40–120). In contrast, the ECA equation performed very well in capturing spatial and temporal variation in the degradation rate (Fig. 3C and D).

3.3. Degradation as a function of both substrate and enzyme concentrations following the ECA model

All cellulose data from each day were averaged over the spatial grid and fitted with the ECA model (Fig. 4). The degradation rate varied significantly with substrate concentration, forming a 'hump-shaped' pattern (Fig. 4A), consistent with Fig. 3A (which shows grid box-specific data from 5 days of a single simulation). Similarly, the degradation rate varied significantly with enzyme concentration, forming a 'closed circle' pattern because of a consistent temporal depletion of substrates (Fig. 4A), also evident in Fig. 3B. It is noteworthy that at the same

enzyme concentration, the degradation rate varied because of the temporal variability in substrate concentration. The ECA equation captured this variation in degradation rate very well as a function of both substrate and enzyme concentration (Fig. 4). The fit of the ECA was robust to variation in the enzyme production rate (Fig. A2 in the Appendix). The ECA fit was also robust across substrates (Fig. A3 and Table A5 in the Appendix).

4. Discussion

4.1. Spatial and temporal variation in substrate degradation rates

Soil systems are highly heterogeneous and dynamically changing; substrate availability, microbial activities, and thereby enzymes are not well-mixed in the soil matrix (e.g., Young and Crawford, 2004; Lowery and Ursell, 2018). This heterogeneity results from many physical, chemical, and biological factors including residue input heterogeneity, physical protection by minerals and aggregation (e.g., Six et al., 2004; Wang et al., 2019), and priming (e.g., Kuzyakov, 2010; Drake et al., 2011). All of these factors contribute to the dynamic, complex interactions of microbial populations and substrate availability, producing heterogeneous degradation in the soil matrix. As in real soil environments, our simulations reflected heterogeneous changes in degradation both temporally and spatially (Fig. 1). Microbes were not uniformly distributed at the onset of simulations, and this heterogeneity was reinforced through reproduction and dispersal. Although DEMENT does
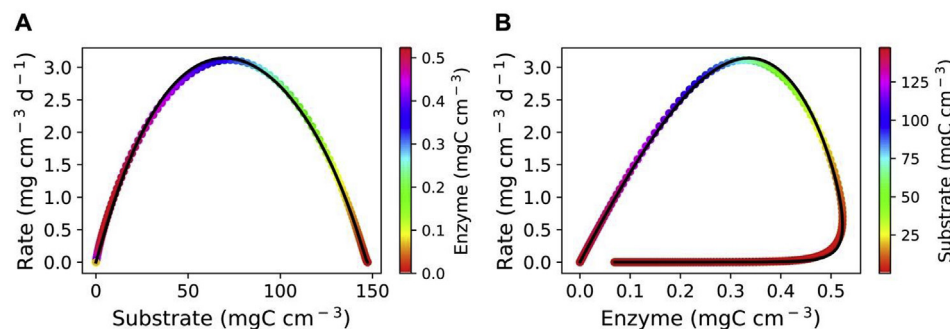

Fig. 4. Cellulose degradation rate as a function of both substrate and enzyme concentration following the ECA model. A) degradation rate versus substrate concentration and **B**) enzyme concentration. Points in color represent averages over the grid for each day with colors denoting enzyme (**A**) or substrate concentration (**B**). Black line follows the fitted ECA equation with $k_2 = 30.7$ mg substrate mg^{-1} enzyme d^{-1} and $k_m = 158.6$ mg cm^{-3} (RMSE = 0.028 mg cm^{-3} d^{-1}). (For interpretation of the references to color in this figure legend, the reader is referred to the Web version of this article.)

not represent all mechanisms leading to heterogeneity in soils, variation in microbial densities was sufficient to drive substantial heterogeneity in substrate concentrations, enzyme concentrations, and degradation rates.

4.2. New kinetic relationships emerge from the forward equation

At the biochemical level, all of our simulations assume forward Michaelis-Menten kinetics for enzyme reactions at a local scale. Within each grid box at a given time step, enzyme and substrate concentrations are assumed to be well-mixed and at steady state. However, at the grid scale and across time steps, these assumptions do not hold (Fig. 2). When new substrates are introduced to an ecosystem, microbial population sizes and enzyme concentrations are low. Microbial cells and enzymes are spatially separated from substrate patches; many patches with high substrate concentrations have zero rates because no enzymes are present locally. Later in the decomposition process, substrate concentrations can decline rapidly, particularly where microbes secrete enzymes and grow rapidly. Within these substrate "holes", the degradation rate per volume or area declines. Therefore the mathematical formulation and parameters used at the scale of a grid box, or applied in a laboratory assay, should not be expected to apply at whole-grid or ecosystem scales.

Still, under certain conditions, emergent kinetics at the grid scale appear to follow the forward or reverse Michaelis-Menten relationships. Early in the decomposition process (Fig. 2B), the degradation rate follows a pseudo-linear increase with enzyme concentration across grid boxes. But as enzyme concentrations increase further, enzymes become locally limited by substrate availability which causes the degradation rate to level off (Fig. 2D). The reverse equation emerges from the local forward kinetics during the early stages of decomposition before substrates become locally depleted. In our simulations, low-enzyme, high substrate conditions persisted for 100–150 days, consistent with a lag in bacterial population growth. Such lags also occur in microcosm experiments during the establishment of pure cultures on sterile, complex substrates (Taylor et al., 1989). In the DEMENT model, lag periods decline as enzyme production rates increase (Fig. A2).

It is noteworthy that this spatial mechanism of rate saturation with enzyme is different from biochemical enzyme kinetics. Biochemically, the reverse equation builds on the assumption of quasi-stationary substrate concentrations, where this assumption is fulfilled for insoluble substrates (interfacial reactions) on which new binding sites are consistently made available to enzymes during degradation (Kari et al., 2017; Andersen et al., 2018). Recently, with cellulose-cellulase as an example system, Kari et al. (2017) showed that the reverse equation is a more applicable kinetic model for enzyme-driven reactions of insoluble substrates.

Later in decomposition, steep declines in substrate concentrations and higher enzyme concentrations (Fig. 1) lead to an emergent forward Michaelis-Menten relationship driven by spatial variation (Fig. 2E). This apparent relationship arises because substrate locally limits microbial activity and enzyme production. Substrate 'holes' have been established long enough for local cell populations to crash and enzyme concentrations to decline. Patches of remaining substrate support higher levels of enzyme production and decay. The timing of emergence for the forward Michaelis-Menten relationship along with the apparent parameters likely depend on enzyme turnover rates (Table A1). In DEMENT, these rates are based on empirical data (Allison, 2006).

4.3. ECA captures kinetics emergent from spatial and temporal variation

Our results show that neither the forward nor the reverse equation can fully describe enzymatic degradation rates in soils (Figs. 2 and 3), whereas the ECA equation is capable of capturing the patterns in substrate degradation over time and space (Figs. 3 and 4). Superficially, this equation makes a very simple linkage to both the forward and reverse equations: when enzyme concentration is low relative to substrate, the equation converges on forward Michaelis-Menten kinetics; when substrate concentration is low relative to enzyme, the equation converges on the reverse equation. Mechanistically, this equation can be derived from the forward and reverse equations based on the law of mass action and the assumption of a quasi-steady state for the enzyme–substrate complex (Tang, 2015; Andersen et al., 2018). Therefore, Tang (2015) concluded that the forward and reverse Michaelis-Menten equations are just two special cases of the ECA based on an analytical analysis. In fact, a similar kinetic description arising from systematic depletion of enzyme and substrate was proposed decades ago by Cha and Cha (1965). Our analyses extend this framework to include apparent kinetics emergent from spatial and temporal variation in enzyme and substrate concentrations, which should be broadly applicable for scaling up microbial processes to the ecosystem scale. This emergence of a coarse-scale pattern from local-scale kinetics is analogous to results from a cell population study by Chaplain et al. (2018), who found that an individual-based model can generate complex spatial patterns of population growth observed in a corresponding continuum model.

4.4. Broder implications for developing soil biogeochemical models

Our study can help develop soil biogeochemical models that more accurately simulate microbe-driven organic matter decomposition and evaluate soil-atmosphere interactions. The spatial and temporal variation in soil systems represents one of the biggest challenges in achieving this goal. To this end, a method for scaling up local heterogeneity is required for large scale modelling. Neither reverse nor forward Michaelis-Menten kinetics are sufficient for this scaling, which may explain the large uncertainties in soil carbon dynamics observed within and across soil carbon models [see the synthesis study by Sulman et al. (2018)]. Our study suggests that the ECA equation is suitable for this scaling process and can be incorporated into land surface and Earth system models (Huang et al., 2018; Riley et al., 2018). ECA parameters can be derived by fitting spatially-explicit model output at the microbial scale (Table A3, A5).

At the same time, a broader application of the ECA requires more attention to the representation of enzymes in ecosystem models. Most current models simulate the enzyme pool implicitly as a function of microbial biomass [see the review by Wieder et al. (2015)]. The ECA may require more explicit parameterizations of enzyme production and activity, a gap that requires more research.

Our study might be generalizable beyond soil systems. Applications of the Michaelis-Menten equation are ubiquitous [e.g., see Table 1 in Wong et al. (2018)], and scaling up the associated processes is a common concern in heterogeneous systems. For example, microbe-driven element cycling in marine systems faces a similar problem of heterogeneity (e.g., Follows et al., 2007; Ward et al., 2013; Moradi et al., 2018), and we speculate that an application of the ECA equation (not necessarily the exact same parameter meaning) could help address this challenge. In forest systems, a landscape mosaic of forest gaps at differing stages (Shugart, 1984) could benefit from a similar application of the ECA equation in a different form.

5. Conclusions

Our model-based analyses shed light on the uncertainty surrounding the enzyme kinetics of litter and soil organic matter decomposition. Specifically, our study shows that both forward and reverse Michaelis-Menten relationships can emerge at the ecosystem scale from local-scale biochemical kinetics. However, these formulations fail to capture the full range of decay rate dependencies on substrate and enzyme concentrations. This inconsistency arises from soil system heterogeneity over space and time that cannot be captured by a single forward or reverse equation. In contrast, we demonstrate that the ECA equation

can represent the emergent spatial and temporal heterogeneity in soil substrate degradation. We expect that adopting this more general equation in building biogeochemical and Earth system models would contribute to greater accuracy in simulating soil carbon metabolism over large scales of time and space.

Acknowledgement

Appendix A. Supplementary data

Supplementary data to this article can be found online at https://doi.org/10.1016/j.soilbio.2019.107522.

References

Allison, S.D., 2006. Soil minerals and humic acids alter enzyme stability: implications for ecosystem processes. Biogeochemistry 81, 361–373.

Allison, S.D., 2012. A trait-based approach for modelling microbial litter decomposition. Ecology Letters 15, 1058–1070.

Allison, S.D., Goulden, M.L., 2017. Consequences of drought tolerance traits for microbial decomposition in the DEMENT model. Soil Biology and Biochemistry 107, 104–113.

Andersen, M., Kari, J., Borch, K., Westh, P., 2018. Michaelis-Menten equation for degradation of insoluble substrate. Mathematical Biosciences 296, 93–97.

Bajzer, Z., Strehler, E.E., 2012. About and beyond the Henri-Michaelis–Menten rate equation for single-substrate enzyme kinetics. Biochemical and Biophysical Research Communications 417, 982–985.

Borghans, J.A., De Boer, R.J., Segel, L.A., 1996. Extending the quasi-steady state approximation by changing variables. Bulletin of Mathematical Biology 58, 43–63.

Cha, S., Cha, C.J.M., 1965. Kinetics of cyclic enzyme systems. Molecular Pharmacology 1, 178–189.

Chaplain, M.A., Macfarlane, F.R., Lorenzi, T., 2018. Bridging the Gap between Individual-Based and Continuum Models of Growing Cell Populations. arXiv preprint arXiv:1812.05872.

Drake, J.E., Gallet-Budynek, A., Hofmockel, K.S., Bernhardt, E.S., Billings, S.A., Jackson, R.B., Johnsen, K.S., Lichter, J., McCarthy, H.R., McCormack, M.L., Moore, D.J., 2011. Increases in the flux of carbon belowground stimulate nitrogen uptake and sustain the long-term enhancement of forest productivity under elevated CO_2. Ecology Letters 14, 349–357.

Follows, M.J., Dutkiewicz, S., Grant, S., Chisholm, S.W., 2007. Emergent biogeography of microbial communities in a model ocean. Science 315, 1843–1846.

Huang, Y., Guenet, B., Ciais, P., Janssens, I.A., Soong, J.L., Wang, Y.L., Goll, D., Blagodatskaya, E., Huang, Y.Y., 2018. ORCHIMIC (v1.0), a microbe-mediated model for soil organic matter decomposition. Geoscientific Model Development 11, 2111–2138.

Kari, J., Andersen, M., Borch, K., Westh, P., 2017. An inverse Michaelis–Menten approach for interfacial enzyme kinetics. ACS Catalysis 7, 4904–4914.

Kuzyakov, Y., 2010. Priming effects: interactions between living and dead organic matter. Soil Biology and Biochemistry 42, 1363–1371.

Lowery, N.V., Ursell, T., 2018. Structured environments fundamentally alter dynamics and stability of ecological communities. In: Proceedings of the National Academy of Sciences, 201811887.

Manzoni, S., Porporato, A., 2009. Soil carbon and nitrogen mineralization: theory and models across scales. Soil Biology and Biochemistry 41, 1355–1379.

Michaelis, L., Menten, M.L., 1913. Die kinetik der invertinwirkung. Biochemische Zeitschrift 49, 333–369.

Monod, J., 1942. Recherches sur la croissance des Cultures Bactériennes. Hermann, Paris.

Moorhead, D.L., Sinsabaugh, R.L., Linkins, A.E., Reynolds, J.F., 1996. Decomposition processes: modelling approaches and applications. The Science of the Total Environment 183, 137–149.

Moorhead, D.L., Lashermes, G., Sinsabaugh, R.L., 2012. A theoretical model of C-and N-acquiring exoenzyme activities, which balances microbial demands during decomposition. Soil Biology and Biochemistry 53, 133–141.

Moorhead, D.L., Weintraub, M.N., 2018. The evolution and application of the reverse Michaelis-Menten equation. Soil Biology and Biochemistry 125, 261–262.

Moradi, N., Liu, B., Iversen, M., Kuypers, M.M., Ploug, H., Khalili, A., 2018. A new mathematical model to explore microbial processes and their constraints in phytoplankton colonies and sinking marine aggregates. Science Advances 4 eaat1991.

Parnas, H., 1975. Model for decomposition of organic material by microorganisms. Soil Biology and Biochemistry 7, 161–169.

Riley, W.J., Zhu, Q., Tang, J.Y., 2018. Weaker land–climate feedbacks from nutrient uptake during photosynthesis-inactive periods. Nature Climate Change 8, 1002–1006.

Roberts, D.V., 1977. Enzyme Kinetics. Cambridge University Press, Cambridge.

Schimel, J.P., Weintraub, M.N., 2003. The implications of exoenzyme activity on microbial carbon and nitrogen limitation in soil: a theoretical model. Soil Biology and Biochemistry 35, 549–563.

Shugart, H.H., 1984. A Theory of Forest Dynamics. Springer Verlag, New York.

Sinsabaugh, R.L., Antibus, R.K., Linkins, A.E., McClaugherty, C.A., Rayburn, L., Repert, D., Weiland, T., 1992. Wood decomposition over a first-order watershed: mass loss as a function of lignocellulase activity. Soil Biology and Biochemistry 24, 743–749.

Sinsabaugh, R.L., Moorhead, D.L., 1994. Resource-allocation to extracellular enzyme production: a model for nitrogen and phosphorus control of litter decomposition. Soil Biology and Biochemistry 26, 1305–1311.

Sinsabaugh, R.L., Lauber, C.L., Weintraub, M.N., Ahmed, B., Allison, S.D., Crenshaw, C., et al., 2008. Stoichiometry of soil enzyme activity at global scale. Ecology Letters 11, 1252–1264.

Six, J., Bossuyt, H., Degryze, S., Denef, K., 2004. A history of research on the link between microaggregates, soil biota, and soil organic matter dynamics. Soil and Tillage Research 79, 7–31.

Sulman, B.N., Moore, J.A., Abramoff, R., Averill, C., Kivlin, S., Georgiou, K., et al., 2018. Multiple models and experiments underscore large uncertainty in soil carbon dynamics. Biogeochemistry 141, 109–123.

Sulman, B.N., Phillips, R.P., Oishi, A.C., Shevliakova, E., Pacala, S.W., 2014. Microbe-driven turnover offsets mineral-mediated storage of soil carbon under elevated CO_2. Nature Climate Change 4, 1099–1102.

Tang, J.Y., 2015. On the relationships between the Michaelis–Menten kinetics, reverse Michaelis–Menten kinetics, equilibrium chemistry approximation kinetics, and quadratic kinetics. Geoscientific Model Development 8, 3823–3835.

Tang, J.Y., Riley, W.J., 2013. A total quasi-steady-state formulation of substrate uptake kinetics in complex networks and an example application to microbial litter decomposition. Biogeosciences 10, 8329–8351.

Taylor, B.R., Parkinson, D., Parsons, W.F., 1989. Nitrogen and lignin content as predictors of litter decay rates: a microcosm test. Ecology 70, 97–104.

Tzafriri, A.R., 2003. Michaelis-Menten kinetics at high enzyme concentrations. Bulletin of Mathematical Biology 65, 1111–1129.

Wang, B., Brewer, P.E., Shugart, H.H., Lerdau, M.T., Allison, S.D., 2019. Soil aggregates as biogeochemical reactors and implications for soil–atmosphere exchange of greenhouse gases—a concept. Global Change Biology 25, 373–385.

Wang, B., Lerdau, M., He, Y., 2017. Widespread production of non-microbial greenhouse gases in soils. Global Change Biology 23, 4472–4482.

Wang, G., Post, W.M., 2013. A note on the reverse Michaelis–Menten kinetics. Soil Biology and Biochemistry 57, 946–949.

Ward, B.A., Dutkiewicz, S., Follows, M.J., 2013. Modelling spatial and temporal patterns in size-structured marine plankton communities: top–down and bottom–up controls. Journal of Plankton Research 36, 31–47.

Wieder, W.R., Allison, S.D., Davidson, E.A., Georgiou, K., Hararuk, O., He, Y., et al., 2015. Explicitly representing soil microbial processes in Earth system models. Global Biogeochemical Cycles 29, 1782–1800.

Wieder, W.R., Grandy, A.S., Kallenbach, C.M., Bonan, G.B., 2014. Integrating microbial physiology and physio-chemical principles in soils with the MIcrobial-MIneral Carbon Stabilization (MIMICS) model. Biogeosciences 11, 3899–3917.

Wong, F., Dutta, A., Chowdhury, D., Gunawardena, J., 2018. Structural conditions on complex networks for the Michaelis–Menten input–output response. Proceedings of the National Academy of Sciences 115, 9738–9743.

Young, I.M., Crawford, J.W., 2004. Interactions and self-organization in the soil-microbe complex. Science 304, 1634–1637.